

EFFECTS OF ADSORBATES ON SUBMONOLAYER GROWTH

MIROSLAV KOTRLA

*Institute of Physics Academy of Sciences of the Czech Republic
Na Slovance 2, 182 21 Praha 8, Czech Republic*

JOACHIM KRUG

*Fachbereich Physik, Universität GH Essen
D-45117 Essen, Germany*

AND

PAVEL ŠMILAUER

*Institute of Physics, Academy of Sciences of the Czech Republic
Čukrovarnická 10, 162 53 Praha 6, Czech Republic*

Abstract. The effects of adsorbates on nucleation and growth of two-dimensional islands is investigated by kinetic Monte Carlo simulations and rate equation theory. The variation of island morphology with adsorbate parameters is discussed and the temperature-dependence of island density in the case of immobile adsorbates is studied in detail. A set of rate equations for the description of nucleation in the presence of predeposited mobile and immobile adsorbates is developed.

1. Introduction

While a satisfactory understanding of nucleation and growth in homoepitaxial systems is beginning to emerge [1], the dramatic effects of tiny traces of adsorbates continue to surprise researchers. Among a wealth of recent examples, we may mention the influence of CO on island shapes and interlayer transport on Pt(111) [2], the modification of attachment kinetics by H preadsorbed on Si(001) [3] and the H-induced enhancement of Pt self-diffusion on Pt(110) [4]. In this situation it seems useful to explore different generic scenarios for adsorbate effects on submonolayer growth within a reasonably simple, yet flexible, theoretical model. The present paper reports on an ongoing effort aimed in this direction.

In Section 2 we briefly review our earlier findings and present new results concerning the dependence of the island density and morphology on the temperature and the characteristics of the adsorbate (mobility and the strength of interaction with adatoms). In the Sec. 3 we sketch a rate equation theory which provides a unified description of two-dimensional nucleation in the presence of predeposited mobile and immobile adsorbates, and derive analytic solutions for some special cases.

2. Kinetic Monte Carlo Simulations

2.1. MODEL

We employ a recently introduced solid-on-solid growth model with two surface species A and B , representing the adatoms of the growing material and the adsorbates, respectively [5, 6]. The simulation starts on a flat substrate composed only of A -atoms. The basic microscopic processes are deposition and migration; desorption is not allowed. Two deposition modes can be studied: (i) simultaneous deposition (*codeposition*) of both species, with generally different fluxes, F_A and F_B , and (ii) *predeposition* of a certain adsorbate coverage θ_B prior to growth.

Adatoms and adsorbates migrate with a nearest-neighbor hopping rate $R_D = k_0 e^{-E_D/k_B T}$, where $k_0 = 10^{13}$ Hz and the energy barrier for a particle of type $X = A$ or B is given by

$$E_D^X = \sum_{Y=A,B} \left(n_0^Y E_{\text{sub}}^{XY} + n_1^{XY} E_n^{XY} \right). \quad (1)$$

Here E_{sub}^{XY} is the hopping barrier for a free X atom on a substrate atom Y , n_0^Y is equal to one if the substrate atom is of type Y and zero otherwise, n_1^{XY} is the number of nearest-neighbor X - Y pairs, and E_n^{XY} is the corresponding contribution to the barrier (symmetric in X and Y). There are no lateral interactions between adsorbate atoms ($E_n^{BB} = 0$). The diffusion rate of a free adatom is $D = k_0 e^{-E_{\text{sub}}^{AA}/k_B T}$.

In previous work [5], we have shown that in addition a process of place exchange between an adsorbate and an adatom with at most one lateral bond is necessary to achieve decorated island edges. This occurs at a rate $k_0 e^{-E_{\text{ex}}/k_B T}$. When the barrier E_{ex} is sufficiently low, then adsorbates are floating on the edges of growing islands.

Adsorbates can be mobile or immobile and strongly or weakly interact with the adatoms. Their mobility is controlled by the strength of interaction of adsorbates with the substrate which is described by the energy barrier E_{sub}^{BA} . The interaction with adatoms is determined by the energy barrier E_n^{AB} .

2.2. SUMMARY OF PREVIOUS RESULTS

We have investigated previously the case of floating mobile adsorbates in the situation when the concentration of adsorbates is comparable with that of the growing material [6]. We studied the dependence of the island density N on the flux F_A and the coverage θ_A for both codeposition and predeposition. We found that the adsorbates strongly increase the island density without appreciably changing its power-law dependence on flux, the increase being stronger for larger E_n^{AB} . The increase was only slightly higher for predeposition than for codeposition.

We also observed a stronger coverage dependence of the island density in comparison with homoepitaxy. This was interpreted as a delay of the saturation regime, where island density becomes independent of coverage. The coverage dependence is again more pronounced for strongly interacting adsorbates, but it is weaker in the case of predeposition than for codeposition. A further noteworthy feature is the much higher density of free adatoms than in homoepitaxy, which shows an intriguing, oscillatory coverage dependence in the case of codeposition [6].

Many of these simulation results could be qualitatively explained in terms of a simple rate equation theory, which rests on the assumption that the adsorbates affect the growth process only by slowing down the diffusion of adatoms. If, in addition, the adsorbates are treated as immobile traps (which may be justified at least for sufficiently high adsorbate coverage θ_B , see Section 3.4), the adatom migration is described by an effective diffusion coefficient

$$\bar{D}(\theta_B) = \frac{D}{1 - \theta_B + \theta_B e^{E_n^{AB}/k_B T}}. \quad (2)$$

Recently, we have considered a situation when only a low concentration of predeposited adsorbates is present on the surface [7]. We investigated the dependence of island density on flux and on the concentration of adsorbates θ_B . Even concentrations as low as $\theta_B = 0.002$ ML can lead to a severalfold increase of the island density. However, the increase significantly depends on the mobility of the adsorbates. In the case of essentially immobile adsorbates ($E_{\text{sub}}^{BA} = 5$ eV), a new feature in the flux dependence of the island density appears. Instead of a single power law relationship, there is a plateau where $N \approx \theta_B$, reflecting the dominance of heterogeneous nucleation in a flux interval $F_1 > F > F_2$. Scaling arguments yield the estimates $F_1 \approx D\theta_B^2$, $F_2 \approx \theta_B D e^{-E_n^{AB}/k_B T}$ for the plateau boundaries in terms of impurity coverage and strength. For sufficiently small θ_B these were confirmed by scaling plots of N/θ_B vs. F/F_1 and F/F_2 [7].

In this work we further extend the above results. In the following subsection, we discuss effects of adsorbates on the island morphology, and in

the subsequent subsection we present results on the temperature dependence of the island density. The energy barriers $E_{\text{sub}}^{AA} = 0.8$ eV, $E_{\text{sub}}^{AB} = 0.1$ eV, $E_{\text{sub}}^{BB} = 0.1$ eV, and $E_n^{AA} = 0.3$ eV were fixed in the following. Other energy barriers as well as the ratio D/F were varied.

2.3. ISLAND MORPHOLOGY

The island shape in homoepitaxy depends on the rates of the various kinetic processes involved. The size of islands varies with the ratio D/F . To be specific, we set in this subsection the temperature to $T = 500$ K. Then, the island shapes in homoepitaxy with the parameters mentioned above in Section 2.2 are regular (approximately rectangular, close to square shape, nondendritic) for fluxes in the interval $F = 0.00025 - 0.64$ ML/s. The shapes become irregular for higher fluxes. In order to evaluate the effect of adsorbates, we performed several sets of simulation with fixed flux $F = 0.001$ ML/s and varying adsorbate properties.

Let us consider first the case of floating adsorbates. It is useful to distinguish two situations: (i) well decorated island and (ii) poorly decorated islands. In the former case, the majority of edge sites is decorated by an adsorbate. We found that the shape is very regular, only the islands are smaller; in fact it can be shown that the decoration *enhances* edge diffusion and thus makes the island edges smoother [6]. The shape is not very sensitive to the mobility of adsorbates. It only has to be sufficiently high so that adsorbates can reach the island edges. The exchange of adatoms approaching the step edge and the adsorbates decorating the step edge is the dominant mechanism.

If the islands are poorly decorated (the number of adsorbates attached to the island edges is considerably less than the number of perimeter sites), then, the shape changes to irregular and regularity is restored again only for very small θ_B . Rather than promoting edge diffusion, in this regime the adsorbates bound on the island edges act as sinks for adatoms provided that the adatom-adsorbate interaction (given by E_n^{AB}) is sufficiently strong. Another factor affecting the island shape in this situation is the change of the mobility of adsorbates (given by E_{sub}^{BA}). Examples of the different island morphologies for various values of parameters E_n^{AB} and E_{sub}^{BA} are shown in Fig. 1. We can see that the increase of both energy barriers leads to more irregular island shapes and also to an increase of island density.

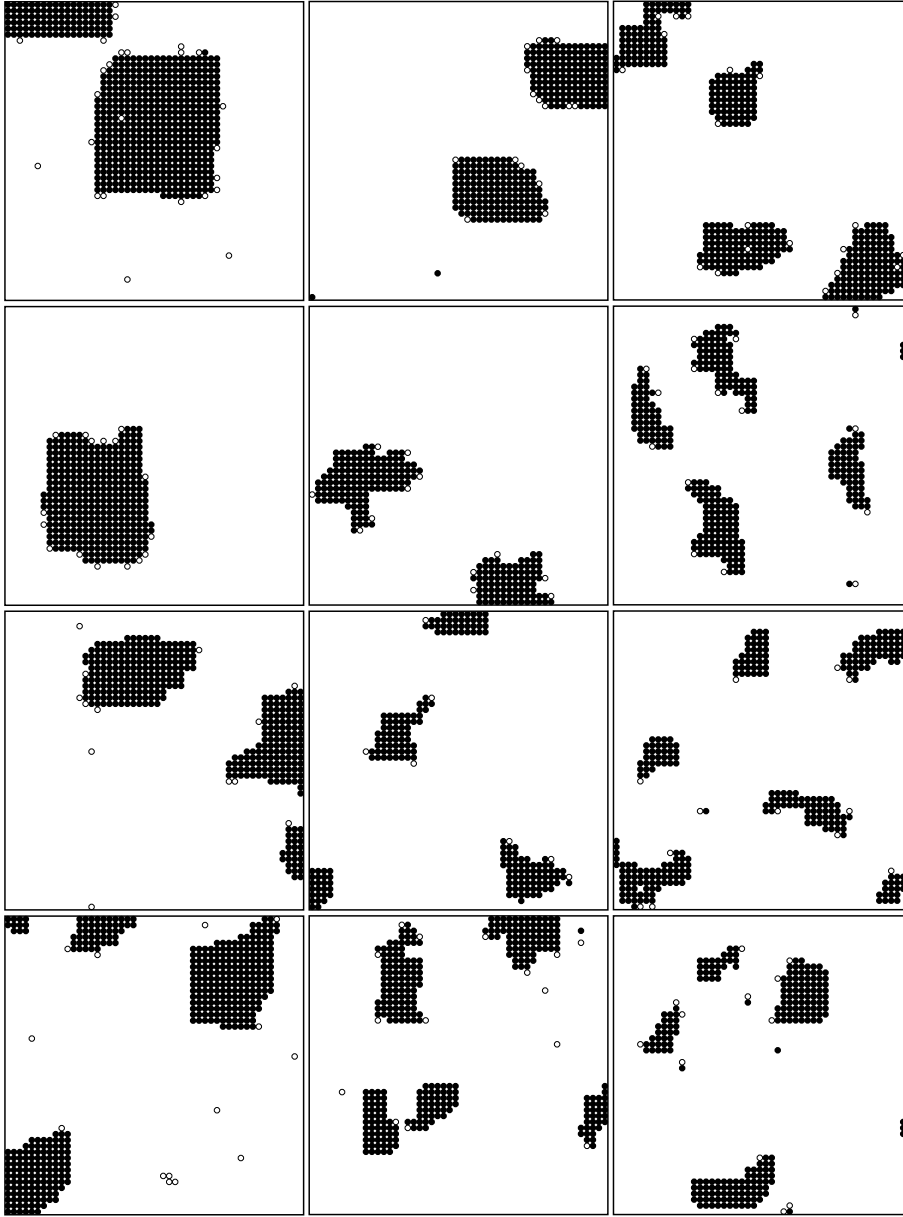


Figure 1. Examples of configurations obtained with flux $F_A = 0.001$ ML/s at a coverage $\theta_A = 0.1$ ML after predeposition $\theta_B = 0.005$ ML of adsorbate coverage, $E_n^{AA} = 0.3$ eV, $E_{\text{ex}} = 1$ eV and different energy barriers $E_n^{AB} = 0.2$ eV (left column), $E_n^{AB} = 0.4$ eV (middle column), $E_n^{AB} = 0.6$ eV (right column), E_{sub}^{BA} : from top to bottom $E_{\text{sub}}^{BA} = 0.7$ eV, $E_{\text{sub}}^{BA} = 1.0$ eV, $E_{\text{sub}}^{BA} = 1.2$ eV, $E_{\text{sub}}^{BA} = 1.5$ eV. We show only 50×50 sections of larger simulation boxes.

The irregularity is not so apparent for weak adsorbate-adatom interaction (left column) or high mobility of adsorbates (top row). The immobile strongly interacting adsorbate catches more diffusing adatoms and at the same time it is floating on the growing island edge. Hence, the island grows faster in the neighborhood of such adsorbates. This kind of adsorbates also block the motion of adatoms along the edge and thus suppresses the smoothening of the island edges.

Let us discuss briefly the island morphology for non-floating adsorbates. The mechanism of floating becomes less relevant for adsorbates with low mobility and does not act at all in the limit of immobile adsorbates. Non-floating adsorbates are incorporated inside a growing island and beyond a certain island size have no effect on growth. In this context, we want to note that surface defects can be treated in our approach as immobile adsorbates.

2.4. TEMPERATURE DEPENDENT ISLAND DENSITY

While in our simulations we have so far focused on the flux dependence of the island density [5-7] in experiments it is most often measured as a function of temperature at fixed flux. Therefore, we complement our previous results by the calculation of the temperature dependence. We restrict ourselves here to the case of predeposition of immobile (non-floating) adsorbates. In Fig.2 we show data for several adsorbate concentrations. We find, similar to the flux dependence [7], a plateau interval $T_1 < T < T_2$, where N is almost independent of T . For low temperatures, $T < T_1$, homogeneous nucleation is more important than heterogeneous nucleation by adsorbates, because the adatoms are not sufficiently mobile to reach the adsorbates. In the plateau region nucleation is predominantly heterogeneous. For high temperatures, $T > T_2$, adatoms start to detach from adsorbates and homogeneous nucleation is again important. This kind of behavior is observed experimentally in defect nucleation on oxide and halide surfaces [8] and in growth on surfaces with strain-relief patterns, which act as an ordered array of defects [9].

For a quantitative estimate of the transition temperatures T_1 and T_2 , we recall the three relevant time scales in the problem [7]: (i) The *diffusion time* $\tau_D \approx 1/D\theta_B$, which is the time required for an atom to explore the “capture zone” of area $1/\theta_B$ associated with a single impurity, and hence to get trapped at the impurity. (ii) The *deposition time* $\tau_F \approx \theta_B/F$, which is the time between subsequent arrivals of adatoms within the capture zone. (iii) The trapping time $\tau \approx (1/D)e^{E_n^{AB}/k_B T}$ at the impurity. The plateau regime is characterized by $\tau > \tau_F > \tau_D$, which yields the expressions

$$T_1 = \frac{E_{\text{sub}}^{AA}}{k_B \ln(k_0 \theta_B^2 / F)}, \quad T_2 = \frac{E_{\text{sub}}^{AA} + E_n^{AB}}{k_B \ln(k_0 \theta_B / F)}. \quad (3)$$

Using $E_{\text{sub}}^{AA} = 0.8$ eV, $F = 0.001$ ML/s and $\theta_B = 0.001$ ML, we get $T_1 = 403$ K, while $T_2 = 465$ K for $E_n^{AB} = 0.4$ eV and $T_2 = 542$ K for $E_n^{AB} = 0.6$ eV, in good agreement with the simulations. From the expression for T_2 , we directly see how the width of the plateau grows with increasing E_n^{AB} .

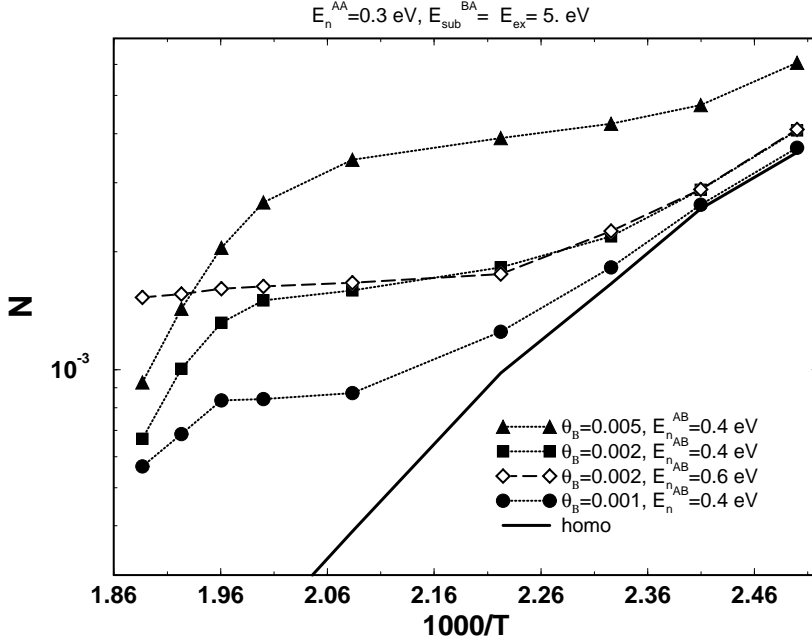


Figure 2. Averaged island density as a function of the inverse temperature for different concentration θ_B of predeposited impurities and different energy of interaction between adsorbates and adatoms: $E_n^{AB} = 0.4$ eV - filled symbols, $E_n^{AB} = 0.6$ eV - open symbols. The adatom interaction energy $E_n^{AA} = 0.3$ eV and the energy barriers $E_{\text{sub}}^{BA} = E_{\text{ex}} = 5$ eV are fixed. Deposition flux is $F_A = 0.001$ ML/s, the coverage of adatoms is $\theta_A = 0.1$ ML. The behavior in the absence of impurities (homoepitaxy, $\theta_B = 0$ ML) is shown for comparison.

3. Rate Equations

In this section we develop a set of rate equations for the description of two-dimensional nucleation in the presence of mobile and immobile adsorbates. Throughout, the impurities will be assumed to have been predeposited at a coverage θ_B , though codeposition is easily incorporated along the lines of our earlier work [6]. To keep matters transparent, we also restrict ourselves to the case of irreversible aggregation (critical nucleus size $i^* = 1$). Detachment of impurities from adatom islands will, however, be included, since this process plays a crucial role at low deposition fluxes.

In addition to the adatom density n and the island density N , a minimal description of nucleation in the presence of adsorbates turns out to require

the monitoring of two additional quantities [8, 10]: The density of free impurities n_0 , and the density n_c of critical clusters bound at impurities; in the present case $i^* = 1$ the latter is simply the density of bound adatom-impurity pairs. Taking into account all relevant processes, one arrives at the following set of evolution equations:

$$dn/dt = F - Dn(2n + N) - Dn(n_0 + n_c) + n_c/\tau, \quad (4)$$

$$dN/dt = Dn(n + n_c), \quad (5)$$

$$dn_0/dt = -Dnn_0 - \tilde{D}n_0N + n_c/\tau + N/\tau', \quad (6)$$

$$dn_c/dt = Dn(n_0 - n_c) - n_c/\tau. \quad (7)$$

Here $1/\tau \approx k_0 e^{-(E_{\text{sub}}^{AA} + E_n^{AB})/k_B T}$ denotes the rate of detachment of an adatom from an impurity, $\tilde{D} = k_0 e^{-E_{\text{sub}}^{BA}/k_B T}$ is the impurity diffusion constant, and $1/\tau' \approx k_0 e^{-(E_{\text{sub}}^{BA} + E_n^{AB})/k_B T}$ is the detachment rate of impurities from islands. In the expression for τ , we have assumed that the impurities are (much) less mobile than the adatoms, so that the relative mobility is dominated by the adatom mobility.

Most of the impurity terms in Eqs.(4-7) should be self-explanatory. We merely point out the term n_c/τ in (4,6,7) which describes the dissociation of adatom-impurity pairs, and the term N/τ' in (7) which describes detachment of impurities from the islands. Strictly speaking, all reaction terms should be adorned with dimensionless capture coefficients. However, since our objective here is a qualitative, rather than a quantitative description, all these coefficients have been set to unity.

3.1. DIMENSIONLESS FORMULATION

Following Tang [11] we now rescale the adatom and island densities by $\sqrt{F/D}$ and time by $1/\sqrt{DF}$. In addition, the impurity densities n_0 and n_c will be rescaled by the initial impurity coverage θ_B . Marking dimensionless quantities with a hat, we obtain the rescaled evolution equations

$$d\hat{n}/d\hat{t} = 1 - \hat{n}(2\hat{n} + \hat{N}) - a\hat{n}(\hat{n}_0 + \hat{n}_c) + b\hat{n}_c, \quad (8)$$

$$d\hat{N}/d\hat{t} = \hat{n}(\hat{n} + a\hat{n}_c), \quad (9)$$

$$d\hat{n}_0/d\hat{t} = -\hat{n}\hat{n}_0 - c\hat{n}_0\hat{N} + (b/a)\hat{n}_c + (bc/a^2)\hat{N}, \quad (10)$$

$$d\hat{n}_c/d\hat{t} = \hat{n}(\hat{n}_0 - \hat{n}_c) - (b/a)\hat{n}_c, \quad (11)$$

where $a = \theta_B \sqrt{D/F}$, $b = \theta_B/F\tau$ and $c = \tilde{D}/D$. The initial conditions are $\hat{n}(0) = \hat{N}(0) = \hat{n}_c(0) = 0$, $\hat{n}_0(0) = 1$.

The parameters a and b may be written in terms of the characteristic fluxes, F_1 and F_2 , which limit the plateau regime in the case of immobile impurities, as $a = \sqrt{F_1/F}$ and $b = F_2/F$. For impurities to be at all relevant, it is necessary that $F_1/F_2 = D\theta_B\tau = a^2/b \gg 1$. By retaining only the most important terms, we can analytically extract the behavior predicted by Eqs.(8-11) in simple cases. So far this has been achieved only for immobile impurities ($c = 0$).

3.2. IMMOBILE IMPURITIES WITHOUT DETACHMENT

Here we consider the plateau regime, where $a \gg 1$ and $b \ll 1$. Numerical integration of (8-11) with $b = c = 0$ and $a \gg 1$ shows that the adatom density is time independent, taking the value $n = F/D\theta_B$ to high accuracy. For early times, this reflects the balance between deposition and capture at impurities, while at late times the capture at islands dominates; since $N = \theta_B$ at late times, the resulting adatom density is the same in both regimes. Setting $n \equiv F/D\theta_B$, the remaining three rate equations become linear and are readily integrated, with the result

$$N = \theta_B(1 - (1 + \theta/\theta_B)e^{-\theta/\theta_B}), \quad (12)$$

$$n_0 = \theta_B e^{-\theta/\theta_B}, \quad (13)$$

$$n_c = \theta e^{-\theta/\theta_B}. \quad (14)$$

Both impurity species decay exponentially at late times.

3.3. IMMOBILE IMPURITIES WITH DETACHMENT

The regime $F \ll F_2$ is detachment-dominated, in the sense that an adatom typically visits many impurities before being incorporated in an island. The primary effect of the impurities is then to slow down the diffusion by temporarily trapping the adatoms [6]. To see how this emerges from the rate equations, we infer from numerical integration that, in the relevant late time regime, an equilibrium is established between attachment and detachment of adatoms at free impurities. This implies that $Dnn_0 \approx n_c/\tau$. Equation (6) then yields $dn_0/dt \approx 0$, so that the impurity concentration essentially retains its initial value $n_0 = \theta_B$, and $n_c \approx (D\theta_B\tau)n$. In this way, the impurity rate equations (6,7) have effectively been eliminated, and we are left with a pair of modified equations for n and N . Taking into account that $D\theta_B\tau = F_1/F_2 \gg 1$, and therefore $n_c \gg n$, they read

$$dn/dt = F - Dn[(D\theta_B\tau)n + N], \quad (15)$$

$$dN/dt = (D\theta_B\tau)Dn^2. \quad (16)$$

Standard analysis [11] shows that the asymptotic island density is of the order $N \sim (F\tau\theta_B)^{1/3}$, which can be brought into the familiar form $N \sim (F/\bar{D})^{1/3}$ by identifying the effective diffusion constant as $\bar{D} = 1/(\tau\theta_B)$. This is precisely the strong impurity limit of (2).

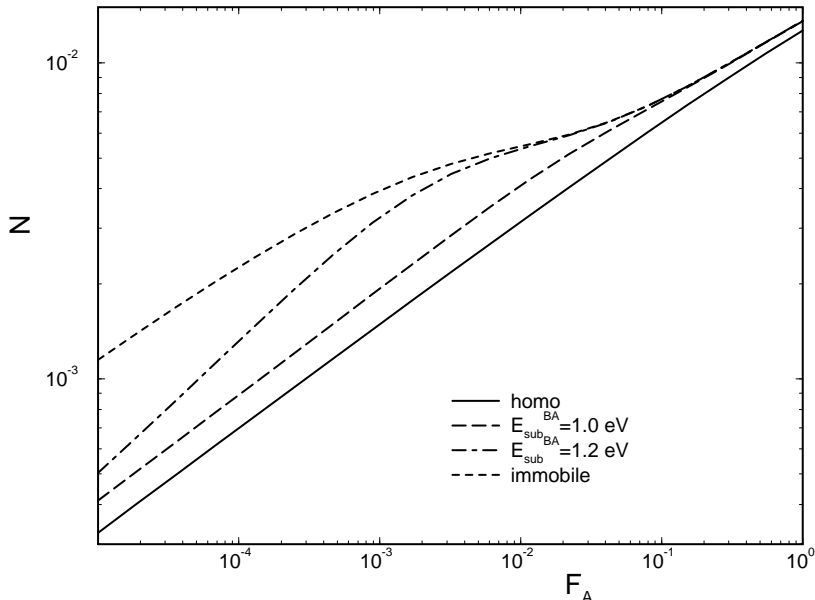


Figure 3. Island density as a function of deposition flux, obtained by numerical solution of the rate equations (4-7) for different choices of the impurity diffusion barrier. The adatom coverage is $\theta = 0.1$ ML and the impurity coverage $\theta_B = 0.005$ ML.

3.4. THE EFFECT OF IMPURITY MOBILITY

The second term on the right-hand side of Equation (6) describes the depletion of free impurities due to capture at stable islands. This is partly compensated by the detachment of impurities from islands described by the last term, but nevertheless, the net effect is expected to be a decrease of the island density, because the depletion reduces the ability of mobile impurities to act as nucleation centers.

In the absence of an analytic study of the full set of rate equations, in Fig. 3 we provide some sample results obtained by numerical integration. The adatom diffusion constant D and the detachment time τ were chosen in accordance with the parameters employed in the KMC simulations. Data for three different choices of the impurity diffusion barrier E_{sub}^{BA} are shown, and the behavior in the absence of impurities is included for reference. The case of low impurity mobility ($E_{\text{sub}}^{BA} = 1.2$ eV, corresponding to $\bar{D}/D \approx 10^{-4}$) is particularly noteworthy, as it indicates an intermediate scaling regime

where the island density scaling exponent, defined by $N \sim F^\chi$, is larger than the homoepitaxial value $\chi = 1/3$ (a fit yields $\chi \approx 0.42$). Further exploration of this phenomenon will be presented elsewhere.

Acknowledgments. J.K. would like to thank CAMP and the Department of Physics at DTU for their kind hospitality while this paper was prepared. Support by the COST project P3.130 and by Volkswagenstiftung are gratefully acknowledged.

References

1. Brune, H. (1998) Microscopic view of epitaxial metal growth: nucleation and aggregation, *Surface Science Reports*, **31**, p. 121–229
2. Kalf, M., Comsa, G. and Michely, T. (1998) How sensitive is epitaxial growth to adsorbates?, *Physical Review Letters*, **81**, pp. 1255–1258
3. Šmilauer, P., Mizushima, K. and Vvedensky D.D. (1998) Activated Si-H exchange at Si-island edges on Si(001), *Physical Review Letters*, **81**, pp. 5600–5603
4. Horch, S., Lorensen, H.T., Helveg, S., Lægsgaard, E., Stensgaard, I., Jacobsen, K.W., Nørskov, J.K. and Besenbacher, F. (1999) Enhancement of surface self-diffusion of platinum atoms by adsorbed hydrogen, *Nature*, **398**, pp. 134–136
5. Kotrla, M., Krug, J. and Šmilauer, P. (2000) Submonolayer growth with decorated island edges, *Surface Science*, **454** – **456**, pp. 681–685
6. Kotrla, M., Krug, J. and Šmilauer, P. (2000) Submonolayer epitaxy with impurities: Kinetic Monte Carlo simulations and rate-equation analysis, *Physical Review B*, **62**, pp. 2889–2898
7. Kotrla, M., Krug, J. and Šmilauer, P. (2000) Effects of mobile and immobile impurities on two-dimensional nucleation, submitted to *Surface Science*
8. Venables, J.A. and Harding, J.H. (2000) Nucleation and growth of supported metal clusters at defect sites on oxide and halide (001) surfaces, *Journal of Crystal Growth*, **211**, pp. 27–33
9. Brune, H., Giovannini, M., Bromann, K. and Kern, K (1998) Self-organized growth of nanostructure arrays on strain-relief patterns, *Nature*, **394**, pp. 451–453
10. Venables, J.A. (1997) Nucleation growth and pattern formation in heteroepitaxy, *Physica A*, **239**, pp. 35–46
11. Tang, L.-H. (1993), Island formation in submonolayer epitaxy, *Journal de Physique I*, **3**, pp. 935–950